Pilot-Free Optimal Control of Linear Systems over OFDM Networks via Control-Aided Channel Prediction

Minjie Tang, Zunqi Li, Marios Kountouris, and Photios A. Stavrou

***Abstract*— Designing optimal controllers for wireless networked control systems (WNCS) typically requires real-time channel state information (CSI), which is difficult to obtain in the presence of time-varying wireless channels. In this work, we propose a pilot-free framework for optimal control over wireless networks, where a linear dynamic plant communicates with a remote controller over an Orthogonal Frequency Division Multiplexing (OFDM) link. The CSI is predicted online from plant states and control inputs using Kalman filtering, thereby eliminating the need for pilot transmissions. Based on the predicted CSI, the control policy is derived using the Bellman principle. To address the resulting curse of dimensionality, we approximate the optimal control solution via a coupled algebraic Riccati equation (CARE), which is solved using a stochastic approximation (SA) algorithm. We establish joint system stability and provide sufficient conditions for the existence, uniqueness, and convergence of the approximate control solution. Simulation results demonstrate that the proposed framework achieves improved control stability performance and channel prediction accuracy compared with widely used baseline methods.**

I. Introduction

The rapid advancements in 5G and edge computing have accelerated the development of wireless networked control systems (WNCSs), where feedback control loops are closed over wireless links [1]. Owing to their flexibility, scalability, and ease of deployment, WNCSs have been widely adopted in domains such as autonomous driving, unmanned aerial vehicle (UAV) swarms, and the industrial Internet of Things (IIoT) [2]. A typical WNCS comprises a dynamic plant with co-located actuators, a remote controller, and a wireless network connecting them, as illustrated in Fig. 1. The controller receives state feedback from the plant and transmits control commands to the actuator through the wireless link to stabilize the system. However, the wireless channels inevitably introduce fading and noise, which challenge control system stability. Achieving optimal stabilizing control thus requires adapting the control policy to the instantaneous channel conditions, which in turn depends on accurate channel state information (CSI). In practice, however, acquiring reliable CSI is difficult due to the stochastic and time-varying nature of wireless channels. This motivates the fundamental question: *Can we design an optimal controller without prior CSI knowledge?*

Minjie Tang and Photios A. Stavrou are with the Department of Communication Systems, EURECOM, France (e-mail: {minjie.tang, fotios.stavrou}@eurecom.fr). Marios Kountouris is with the Department of Communication Systems, EURECOM, France, and the Department of Computer Science and Artificial Intelligence, University of Granada, Spain (e-mails: marios.kountouris@eurecom.fr;mariosk@ugr.es). Zunqi Li is with the School of Electronics and Information Engineering, Harbin Institute of Technology, Harbin, China and National Key Laboratory of Advanced Communication Networks, Shijiazhuang, China (e-mail: lizunqi@stu.hit.edu.cn).

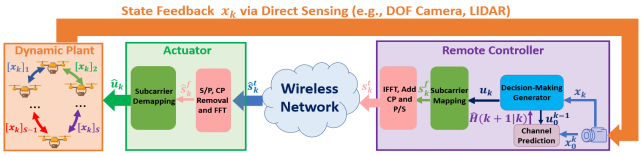

Fig. 1: A typical architecture of the WNCS under the pilot-free framework.

Most controller design methods assume static or simplified communication channels. For instance, proportional–integral–derivative (PID) control [3] is widely used but requires extensive tuning, while more principled approaches such as linear quadratic regulator (LQR) [4] and model predictive control (MPC) [5] achieve optimality under idealized links. In practical WNCSs operating over unreliable wireless channels, however, their performance often degrades significantly. To enhance robustness, simplified channel models—such as additive white Gaussian noise (AWGN) [6], packet drops [7], and finite-state Markov losses [8]—are often adopted, but they fail to capture temporal correlation and continuous fading in real wireless environments. Although recent works such as [9] consider fading channels, they typically rely on independent and identically distributed (i.i.d.) or finite-state assumptions and assume perfect CSI [7]–[9], which is unrealistic in fast-varying systems.

Accurate CSI acquisition typically relies on explicit estimation or prediction. To achieve this goal, conventional pilot-aided methods [10] have been widely adopted, where predefined pilot sequences are transmitted for channel estimation, followed by CSI feedback to enable control optimization. However, such approaches incur significant spectral and energy overhead, especially in massive multiple-input multiple-output (MIMO) systems due to pilot contamination. To alleviate this, alternatives including blind [11], semi-blind [12], compressed sensing (CS)–based [13], and deep learning (DL)–based approaches [14] have been proposed. Blind and semi-blind methods reduce pilot dependence but suffer from slow convergence and high complexity. CS lowers overhead via channel sparsity yet is sensitive to noise and model mismatch, while DL methods [15] capture nonlinear dynamics but require large labeled datasets, limiting adaptability.

In this work, we propose a pilot-free optimal control framework for linear systems over orthogonal frequency-division multiplexing (OFDM) networks. The framework captures temporal channel correlation and high-dimensional fading induced by multipath propagation, and thereby re-

flecting realistic wireless conditions. The key idea is to use control signals to simultaneously regulate the system and enable control-aided channel prediction from real-time plant states, eliminating the need for prior CSI. The main contributions are summarized below:

1) We propose a *pilot-free framework for WNCSs*. Unlike existing works that either separate control and channel prediction or rely on perfect or pilot-based CSI [16], our approach reuses real-time control signals as implicit pilots for channel prediction. To the best of our knowledge, this is the first work to exploit control signals for channel learning, enabling pilot-free controller design that removes the need for prior CSI and reduces communication overhead while preserving control stability performance.
2) We formulate and solve a *pilot-free optimal control problem for linear systems over an OFDM network*, where we jointly optimize channel prediction and system control. Specifically, channel prediction is performed via the Kalman filter [17], while control policy is derived using the Bellman principle [18]. To address the curse of dimensionality, we propose a statistical quantization–based approximation that leads to a coupled algebraic Riccati equation (CARE). The control policy is then approximately obtained via an efficient stochastic approximation (SA)–based online algorithm that leverages control-aided channel prediction.
3) We establish *rigorous performance guarantees* for the proposed pilot-free framework, including: (i) stability of both the channel prediction and the dynamic plant under the optimal solution, (ii) sufficient conditions for the existence and uniqueness of a stabilizing solution to the CARE, and (iii) convergence of the proposed SA-based online control algorithm.

Notation: Uppercase and lowercase boldface letters denote matrices and vectors, respectively. The operators $(\cdot)^T$, $(\cdot)^H$, and $\mathrm{Tr}(\cdot)$ denote transpose, Hermitian transpose, and trace. The symbols $\mathbf{0}_{m\times n}$, $\mathbf{0}_m$, and $\mathbf{I}_m$ denote the $m \times n$ zero matrix, $m \times m$ zero matrix, and $m \times m$ identity matrix, respectively. For $(a_1, \ldots, a_n)$, $\mathrm{Diag}(a_1, \ldots, a_n)$ denotes the diagonal matrix with entries $a_1, \ldots, a_n$. The sets $\mathbb{R}^{m\times n}$ and $\mathbb{C}^{m\times n}$ denote real and complex matrices; $\mathbb{S}^m_+$ and $\mathbb{S}^m_{++}$ denote positive semidefinite and positive definite matrices; $\mathbb{Z}_+$ denotes nonnegative integers; and $\mathbb{R}$ and $\mathbb{C}$ denote real and complex numbers. The norms $\|\mathbf{A}\|$, $\|\mathbf{A}\|_F$, and $\|\mathbf{a}\|$ denote the spectral, Frobenius, and Euclidean norms, respectively, while $\|\cdot\|_0$ counts the number of nonzero entries. For a matrix $\mathbf{A}$, $[\mathbf{A}]_{i,:}$ and $[\mathbf{A}]_{:,i}$ denote its ith row and column, and for a vector $\mathbf{a}$, $[\mathbf{a}]_i$ denotes its ith entry.

II. System Model

A. Decision-Making at the Dynamic Plant

We consider the discrete-time system in Fig. 1, where the state $\mathbf{x}_k \in \mathbb{C}^{S\times 1}$ evolves according to a first-order linear difference equation:

$$\mathbf{x}_{k+1} = \mathbf{A}\mathbf{x}_k + \mathbf{B}\widehat{\mathbf{u}}_k + \mathbf{w}_k, \quad k = 0, 1, 2, \ldots. \tag{1}$$

The initial state $\mathbf{x}_0$ is assumed to follow a complex Gaussian distribution with zero mean and covariance matrix $\sigma_x^2\mathbf{I}_S$, i.e., $\mathbf{x}_0 \sim \mathcal{CN}(\mathbf{0}, \sigma_x^2\mathbf{I}_S)$. The received control signal is $\widehat{\mathbf{u}}_k \in \mathbb{C}^{N\times 1}$. $\mathbf{A} \in \mathbb{R}^{S\times S}$ and $\mathbf{B} \in \mathbb{R}^{S\times N}$ denote the system and actuation matrices, respectively. The process noise $\mathbf{w}_k \sim \mathcal{CN}(\mathbf{0}, \mathbf{W})$ has covariance $\mathbf{W} \in \mathbb{S}^S_+$, and $(\mathbf{A}, \mathbf{B})$ is controllable.[1]

B. Signal Processing at Remote Controller

The remote controller monitors the real-time plant state history $\mathbf{x}_0^k = \{\mathbf{x}_0, \ldots, \mathbf{x}_k\}$ using a depth camera, and simultaneously performs channel prediction based on both the observed states $\mathbf{x}_0^k$ and the control command history $\mathbf{u}_0^{k-1} = \{\mathbf{u}_0, \ldots, \mathbf{u}_{k-1}\}$. The predicted wireless fading gain at each time slot k is represented as

$$\widehat{\mathbf{H}}(k+1|k) = f_{\text{pred}}(\mathbf{x}_0^k, \mathbf{u}_0^{k-1}), \tag{2}$$

where $f_{\text{pred}}(\cdot)$ denotes the channel prediction operator, whose specific form will be detailed in Section III. The predicted fading matrix $\widehat{\mathbf{H}}(k+1|k) \in \mathbb{C}^{N\times N}$ is diagonal and constructed as $\widehat{\mathbf{H}}(k+1|k) = \mathrm{Diag}(\widehat{\mathbf{h}}(k+1|k))$, where $\widehat{\mathbf{h}}(k+1|k) = [[\widehat{\mathbf{h}}(k+1|k)]_1, \ldots, [\widehat{\mathbf{h}}(k+1|k)]_N]^T$ and $[\widehat{\mathbf{h}}(k+1|k)]_i$ is the predicted fading gain on the i-th subcarrier.

The control command $\mathbf{u}_k \in \mathbb{C}^{N\times 1}$ is generated from the observed state history $\mathbf{x}_0^k$ and the control command history $\mathbf{u}_0^{k-1}$ as

$$\mathbf{u}_k = f_{\text{cont}}(\mathbf{x}_0^k, \mathbf{u}_0^{k-1}), \tag{3}$$

where $f_{\text{cont}}(\cdot)$ denotes the control policy, whose specific form will be described in Section III.

The control command $\mathbf{u}_k$ is mapped to predetermined subcarriers in the frequency domain according to $\mathbf{s}_k^f = \mathbf{P}\mathbf{u}_k$, resulting in $\mathbf{s}_k^f \in \mathbb{C}^{N\times 1}$. This mapping follows a fixed and disjoint subcarrier assignment, where each component $[\mathbf{u}_k]_i$ is associated with a unique subcarrier without any overlap. The subcarrier allocation is characterized by a binary matrix $\mathbf{P} \in \{0, 1\}^{N\times N}$ that satisfies three constraints: (i) *Bandwidth utilization*: $\|\mathbf{P}\|_0 = N$, ensuring full utilization of the available subcarriers; (ii) *Disjoint mapping*: $[\mathbf{P}]_{:,i}^T[\mathbf{P}]_{:,j} = 0$ for all $i \neq j$, guaranteeing non-overlapping subcarrier assignments among control components; and (iii) *Bijective mapping*: $\|[\mathbf{P}]_{:,i}\|_0 = \|[\mathbf{P}]_{j,:}\|_0 = 1$ for all $i, j \in \{1, \ldots, N\}$, ensuring a one-to-one correspondence between signal components and subcarriers.

The frequency-domain symbol vector $\mathbf{s}_k^f \in \mathbb{C}^{N\times 1}$ is converted into a time-domain block $\tilde{\mathbf{s}}_k^t = \mathbf{F}^H\mathbf{s}_k^f$ using the inverse fast Fourier transform (IFFT), where $\mathbf{F} \in \mathbb{C}^{N\times N}$ denotes the unitary fast Fourier transform (FFT) matrix. To mitigate inter-symbol interference (ISI) caused by multipath fading, a cyclic prefix (CP) of length L_{cp} is appended by copying the last L_{cp} samples of $\tilde{\mathbf{s}}_k^t$ to the beginning of the block, yielding the CP-extended vector $\mathbf{s}_k^t \in \mathbb{C}^{(N+L_{\text{cp}})\times 1}$.

[1]The state $\mathbf{x}_k$, control signal $\mathbf{u}_k$, received signal $\widehat{\mathbf{u}}_k$, and channel matrices $\mathbf{H}_k$ and $\mathbf{H}_k^c$ are modeled as complex-valued to capture baseband wireless transmission [10].

The resulting block then undergoes parallel-to-serial conversion and RF processing before being transmitted over the wireless channel to the dynamic plant.

C. Signal Processing at the Dynamic Plant

The received serial signal is converted into a parallel block via a serial-to-parallel (S/P) conversion, yielding[2]

$$\widehat{\mathbf{s}}_k^t = \mathbf{H}_{k+1}^t \mathbf{s}_k^t + \mathbf{n}_k^t, \tag{4}$$

where $\mathbf{H}_{k+1}^t \in \mathbb{C}^{(N+L_{\text{cp}})\times(N+L_{\text{cp}})}$ denotes the Toeplitz convolution matrix induced by the channel impulse response $\mathbf{h}_{k+1}^t = [h_{0,k+1}^t, \ldots, h_{L_h-1,k+1}^t]^T \in \mathbb{C}^{L_h\times 1}$, with L_h being the effective channel length, and $\mathbf{n}_k^t \sim \mathcal{CN}(\mathbf{0}_{N+L_{\text{cp}}}, \sigma_n^2 \mathbf{I}_{N+L_{\text{cp}}})$ denoting additive white Gaussian noise (AWGN) in the time domain.

After removing the first L_{cp} cyclic prefix samples, the effective N-point received vector is given by

$$\widehat{\mathbf{s}}_k^r = \mathbf{R}\,\widehat{\mathbf{s}}_k^t = \mathbf{H}_{k+1}^{\text{circ}} \tilde{\mathbf{s}}_k^t + \tilde{\mathbf{n}}_k^t, \tag{5}$$

where $\mathbf{R} \in \{0,1\}^{N\times(N+L_{\text{cp}})}$ is a selection matrix that removes the CP by extracting the last N entries of the received block. $\mathbf{H}_{k+1}^{\text{circ}} = \mathbf{R}\mathbf{H}_{k+1}^t \in \mathbb{C}^{N\times N}$ denotes the circulant convolution matrix generated from $\mathbf{h}_{k+1}^t$, and $\tilde{\mathbf{n}}_k^t \sim \mathcal{CN}(\mathbf{0}_{N\times 1}, \sigma_n^2 \mathbf{I}_N)$ represents the AWGN vector after CP removal.

Applying the fast Fourier transform (FFT) to $\widehat{\mathbf{s}}_k^r$ yields

$$\widehat{\mathbf{s}}_k^f = \mathbf{F}\widehat{\mathbf{s}}_k^r = \mathbf{H}_{k+1}\mathbf{s}_k^f + \mathbf{n}_k, \tag{6}$$

where $\mathbf{F} \in \mathbb{C}^{N\times N}$ is the unitary FFT matrix, and $\mathbf{n}_k \sim \mathcal{CN}(\mathbf{0}_{N\times 1}, \sigma_n^2 \mathbf{I}_N)$ denotes frequency-domain AWGN. The channel matrix is given by $\mathbf{H}_{k+1} = \mathbf{F}\mathbf{H}_{k+1}^{\text{circ}}\mathbf{F}^H = \text{Diag}(h_{1,k+1}, \ldots, h_{N,k+1}) \in \mathbb{C}^{N\times N}$, where each subcarrier gain $h_{i,k+1} \in \mathbb{C}$ evolves as a Gauss–Markov process [19]

$$h_{i,k+1} = \alpha h_{i,k} + \sqrt{1-\alpha^2} v_{i,k}, \tag{7}$$

with $h_{i,0} \sim \mathcal{CN}(0,1)$. $\alpha \in [-1,1]$ denotes the temporal correlation coefficient of the Gauss-Markov fading process. $v_{i,k} \sim \mathcal{CN}(0,\sigma_v^2)$ is the i.i.d. complex Gaussian noise.

The dynamic plant recovers the control command $\widehat{\mathbf{u}}_k \in \mathbb{C}^{N\times 1}$ from $\widehat{\mathbf{s}}_k^f$ as

$$\widehat{\mathbf{u}}_k = \mathbf{P}^T \widehat{\mathbf{s}}_k^f = \mathbf{H}_{k+1}^c \mathbf{u}_k + \mathbf{n}_k^c, \tag{8}$$

where $\mathbf{H}_{k+1}^c = \mathbf{P}^T \mathbf{H}_{k+1} \mathbf{P}$ and $\mathbf{n}_k^c = \mathbf{P}^T \mathbf{n}_k$. The recovered control command $\widehat{\mathbf{u}}_k$ is then applied to the dynamic plant, as described in Section II-A.

D. Pilot-Free Communication Paradigm for the WNCS

The models in Sections II-A–II-C introduce a pilot-free communication paradigm for WNCSs, where the control signal $\mathbf{u}_k$ both drives the plant state $\mathbf{x}_k$ and enables implicit prediction of $\mathbf{H}_{k+1}$ by exploiting the relation among $\mathbf{x}_k$, $\mathbf{u}_k$, and its noisy observation $\widehat{\mathbf{u}}_k$. Specifically, the controller generates $\mathbf{u}_k$ via $f_{\text{cont}}(\mathbf{x}_0^k, \mathbf{u}_0^{k-1})$, while channel prediction follows $f_{\text{pred}}(\mathbf{x}_0^k, \mathbf{u}_0^{k-1})$. Unlike conventional WNCSs relying on perfect CSI or pilot transmissions [9], the proposed framework reuses control signals for implicit channel learning, thereby reducing signaling overhead and improving spectral and energy efficiency.

[2]We consider analog communication from the controller to the plant, accounting for fading $\mathbf{H}_k^t$ and noise $\mathbf{n}_k^t$, which avoids encoding/decoding and simplifies the system architecture compared to digital schemes.

III. Channel Prediction and Optimal Control

A. Problem Formulation

The channel prediction policy $\pi^p = \left\{\widehat{\mathbf{H}}(1|0), \widehat{\mathbf{H}}(2|1), \ldots\right\}$ seeks to produce accurate estimates of $\mathbf{H}_k^c$, leading to the following optimization problem.

Problem 1 (Channel Prediction Problem):

$$\min_{\substack{\pi^p \\ (1)\text{–}(8)}} \limsup_{K\to\infty} \frac{1}{K} \sum_{k=0}^{K-1} \mathbb{E}[c_p(\widehat{\mathbf{H}}(k+1|k), \mathbf{H}_{k+1}^c) \mid \mathbf{x}_0^k, \mathbf{u}_0^{k-1}],$$

where the per-stage cost is defined as $c_p(\widehat{\mathbf{H}}(k+1|k), \mathbf{H}_{k+1}^c) \triangleq \|\widehat{\mathbf{H}}(k+1|k) - \mathbf{H}_{k+1}^c\|_F^2$.

The control policy $\pi^c = \{\mathbf{u}_0, \mathbf{u}_1, \ldots\}$ aims to stabilize the dynamic plant, and is obtained by solving the following optimization problem.

Problem 2 (Optimal Control Problem):

$$\min_{\substack{\pi^c \\ (1)\text{–}(8)}} \limsup_{K\to\infty} \frac{1}{K} \sum_{k=0}^{K-1} \mathbb{E}\left[c_d(\mathbf{x}_k, \mathbf{u}_k)\right], \tag{9}$$

where per-stage cost $c_d(\mathbf{x}_k, \mathbf{u}_k) \triangleq \mathbf{x}_k^H \mathbf{Q} \mathbf{x}_k + \mathbf{u}_k^H \mathbf{R} \mathbf{u}_k$. $\mathbf{Q} \in \mathbb{S}_+^S, \mathbf{R} \in \mathbb{S}_+^N$ are weighting matrices.

B. Solution to Problem 1

The optimal solution to Problem 1 corresponds to the minimum mean square error (MMSE) prediction of $\mathbf{H}_{k+1}^c$ at each time slot, given by $\widehat{\mathbf{H}}(k+1|k) = \arg\min_{\widehat{\mathbf{H}}(k+1|k)} \mathbb{E}[\|\widehat{\mathbf{H}}(k+1|k) - \mathbf{H}_{k+1}^c\|_F^2 \,|\, \mathbf{x}_0^k, \mathbf{u}_0^{k-1}]$. To derive the explicit form of the optimal predictor, we combine (1) with (8), yielding

$$\mathbf{x}_k = \mathbf{A}\mathbf{x}_{k-1} + \mathbf{B}\mathbf{U}_{k-1}\mathbf{h}_k^c + \mathbf{B}\mathbf{n}_{k-1}^c + \mathbf{w}_k, \tag{10}$$

where $\mathbf{U}_k = \text{Diag}\left([\mathbf{u}_k]_1, \ldots, [\mathbf{u}_k]_N\right) \in \mathbb{C}^{N\times N}$ denotes the diagonalized control signal, and $\mathbf{h}_k^c = [[\mathbf{H}_k^c]_{1,1}, [\mathbf{H}_k^c]_{2,2}, \ldots, [\mathbf{H}_k^c]_{N,N}]^T \in \mathbb{C}^{N\times 1}$ represents the vectorized channel gain with the channel dynamics

$$\mathbf{h}_{k+1}^c = \alpha \mathbf{h}_k^c + \mathbf{v}_k, \tag{11}$$

where $\mathbf{v}_k \in \mathbb{C}^{N\times 1}$ collects the innovation terms, with entries $[\mathbf{v}_k]_i = \sqrt{1-\alpha^2}\, v_{i,k}$ for $i \in \{1, \ldots, N\}$.

Based on (10) and (11) , Problem 1 reduces to an MMSE prediction problem for $\mathbf{h}_k^c$, which can be optimally solved using the KF algorithm.

Specifically, we denote the posterior and prior channel estimates as $\widehat{\mathbf{h}}(k|k) = \mathbb{E}[\mathbf{h}_k^c \,|\, \mathbf{x}_0^k, \mathbf{U}_0^{k-1}]$ and $\widehat{\mathbf{h}}(k|k-1) = \mathbb{E}[\mathbf{h}_k^c \,|\, \mathbf{x}_0^{k-1}, \mathbf{U}_0^{k-2}]$, respectively. The corresponding error covariances are $\Sigma(k|k) = \mathbb{E}[(\mathbf{h}_k^c - \widehat{\mathbf{h}}(k|k))(\mathbf{h}_k^c - \widehat{\mathbf{h}}(k|k))^H \,|\, \mathbf{x}_0^k, \mathbf{U}_0^{k-1}]$ and $\Sigma(k|k-1) = \mathbb{E}[(\mathbf{h}_k^c - \widehat{\mathbf{h}}(k|k-1))(\mathbf{h}_k^c - \widehat{\mathbf{h}}(k|k-1))^H \,|\, \mathbf{x}_0^{k-1}, \mathbf{U}_0^{k-2}]$. Assume that the initial channel prediction is distributed as $\widehat{\mathbf{h}}(1|0) \sim$

Algorithm 1 Pilot-free MMSE Channel Prediction

Initialization:
  Set initial prior error covariance $\Sigma(1|0) = \mathbf{I}_N$
  Generate $\widehat{\mathbf{h}}(1|0) \sim \mathcal{CN}(\mathbf{0}_{N\times 1}, \Sigma(1|0))$
for $k = 1, 2, \ldots$ **do**
  Construct $\mathbf{U}_{k-1} = \mathrm{Diag}([\mathbf{u}_{k-1}]_1, \ldots, [\mathbf{u}_{k-1}]_N)$,
  where $\mathbf{u}_{k-1}$ is from Algorithm 2
  • **Estimation Step (for $\mathbf{h}^c_k$):**
  $\mathbf{K}_k = \Sigma(k|k-1)\mathbf{U}^H_{k-1}\mathbf{B}^T(\mathbf{B}\mathbf{U}_{k-1}\Sigma(k|k-1)$
  $\mathbf{U}^H_{k-1}\mathbf{B}^T + \sigma_n^2\mathbf{B}\mathbf{B}^T + \mathbf{W})^{-1}$,
  $\widehat{\mathbf{h}}(k|k) = \widehat{\mathbf{h}}(k|k-1) + \mathbf{K}_k(\mathbf{x}_k - \mathbf{A}\mathbf{x}_{k-1} - \mathbf{B}\mathbf{U}_{k-1}$
  $\times\widehat{\mathbf{h}}(k|k-1))$,
  $\Sigma(k|k) = (\mathbf{I}_N - \mathbf{K}_k\mathbf{B}\mathbf{U}_{k-1})\Sigma(k|k-1)$
  $\times(\mathbf{I}_N - \mathbf{K}_k\mathbf{B}\mathbf{U}_{k-1})^H + \mathbf{K}_k(\sigma_n^2\mathbf{B}\mathbf{B}^T + \mathbf{W})\mathbf{K}_k^H$.
  • **Prediction Step (for $\mathbf{h}^c_{k+1}$):**
  $\widehat{\mathbf{h}}(k+1|k) = \alpha\widehat{\mathbf{h}}(k|k)$,
  $\Sigma(k+1|k) = \alpha^2\Sigma(k|k) + \mathbf{V}$,
  where $\mathbf{V} = \sigma_v^2\,\mathrm{Diag}(1-\alpha^2, \ldots, 1-\alpha^2) \in \mathbb{C}^{N\times N}$.
end for

$\mathcal{CN}(\mathbf{0}_{N\times 1}, \mathbf{I}_N)$. Then, the optimal solution to Problem 1 is given by $\widehat{\mathbf{H}}(k+1|k) = \arg\min_{\widehat{\mathbf{H}}} \mathbb{E}[\|\widehat{\mathbf{H}} - \mathbf{H}^c_{k+1}\|_F^2 \,|\, \mathbf{x}_0^k, \mathbf{u}_0^{k-1}] = \mathrm{Diag}([\widehat{\mathbf{h}}(k+1|k)]_1, \ldots, [\widehat{\mathbf{h}}(k+1|k)]_N)$, where $\widehat{\mathbf{h}}(k+1|k)$ denotes the Kalman prediction generated by Algorithm 1.

We now analyze the channel prediction stability based on Algorithm 1, as stated below.

Theorem 1 (Stability of Channel Prediction): Under (10) and (11), $\Sigma(k+1|k)$ generated by Algorithm 1 is mean-square stable, i.e., $\limsup_{K\to\infty}\frac{1}{K}\sum_{k=0}^{K-1}\mathbb{E}[\mathrm{Tr}(\Sigma(k+1|k))] < \frac{\sigma_v^2 N}{1-\alpha^2}\mathbf{1}_{|\alpha|<1} + N\mathbf{1}_{|\alpha|=1} < \infty$.

Proof: The proof is given in [20, see Theorem 1]. ■

C. Solution to Problem 2

Let $\widehat{\mathbf{H}}(k+1|k) = \mathrm{Diag}([\widehat{\mathbf{h}}(k+1|k)]_1, \ldots, [\widehat{\mathbf{h}}(k+1|k)]_N) \in \mathbb{C}^{N\times N}$ denote the predicted channel gain at the k-th time slot. The optimal solution to Problem 2 can be equivalently formulated by means of a Markov-modulated (MM) Bellman optimality equation, as follows.

Theorem 2 (MM Bellman Equation): If, for each predicted channel state $\widehat{\mathbf{H}}(k+1|k)$, there exists a unique positive semidefinite matrix $\mathbf{P}(\widehat{\mathbf{H}}(k+1|k)) \in \mathbb{S}_+^S$ that satisfies:

$$\begin{aligned}\mathbf{P}(\widehat{\mathbf{H}}(k+1|k)) &= \mathbf{Q} + \mathbf{A}^T\mathbf{P}(\alpha\widehat{\mathbf{H}}(k+1|k))\mathbf{A}\\ &- \mathbf{A}^T\mathbf{P}(\alpha\widehat{\mathbf{H}}(k+1|k))\mathbf{B}\widehat{\mathbf{H}}(k+1|k)((\widehat{\mathbf{H}}(k+1|k))^H\mathbf{B}^T\\ &\times\mathbf{P}(\alpha\widehat{\mathbf{H}}(k+1|k))\mathbf{B}\widehat{\mathbf{H}}(k+1|k) + \mathbf{R} + \mathrm{Tr}(\mathbf{B}^T\\ &\times\mathbf{P}(\alpha\widehat{\mathbf{H}}(k+1|k))\mathbf{B}\Sigma(k+1|k))\mathbf{I}_N)^{-1}(\widehat{\mathbf{H}}(k+1|k))^H\\ &\times\mathbf{B}^T\mathbf{P}(\alpha\widehat{\mathbf{H}}(k+1|k))\mathbf{A}, \end{aligned}\tag{12}$$

then the optimal solution to Problem 2 can be characterized by the following MM Bellman optimality equation.

$$\begin{aligned}\rho(\widehat{\mathbf{H}}(k+1|k)) + V(\mathbf{x}_k, \widehat{\mathbf{H}}(k+1|k)) &= \min_{\mathbf{u}_k}\ \mathbb{E}[c_d(\mathbf{x}_k, \mathbf{u}_k)\\ &+ V(\mathbf{x}_{k+1}, \widehat{\mathbf{H}}(k+2|k+1)) \,|\, \mathbf{x}_k, \widehat{\mathbf{H}}(k+1|k), \mathbf{u}_k], \end{aligned}\tag{13}$$

where $\rho(\widehat{\mathbf{H}}(k+1|k)) = \mathrm{Tr}(\sigma_n^2\mathbf{B}^T\mathbf{P}(\alpha\widehat{\mathbf{H}}(k+1|k))\mathbf{B} + \mathbf{P}(\alpha\widehat{\mathbf{H}}(k+1|k))\mathbf{W})$ denotes the per-stage bias, and $\limsup_{K\to\infty}\frac{1}{K}\sum_{k=0}^{K-1}\mathbb{E}[\rho(\widehat{\mathbf{H}}(k+1|k))]$ represents the optimal cost associated with Problem 2. $V(\mathbf{x}_k, \widehat{\mathbf{H}}(k+1|k)) = \mathbf{x}_k^H\mathbf{P}(\widehat{\mathbf{H}}(k+1|k))\mathbf{x}_k$ denotes the value function over the plant state $\mathbf{x}_k$ and the predicted channel state $\widehat{\mathbf{H}}(k+1|k)$. Moreover, the optimal control action $\mathbf{u}_k^*$ that minimizes the right-hand side (RHS) of the Bellman equation (13) is given by

$$\begin{aligned}\mathbf{u}_k^* &= -(\mathbf{R} + (\widehat{\mathbf{H}}(k+1|k))^H\mathbf{B}^T\mathbf{P}(\alpha\widehat{\mathbf{H}}(k+1|k))\mathbf{B}\\ &\times\widehat{\mathbf{H}}(k+1|k) + \mathrm{Tr}(\mathbf{B}^T\mathbf{P}(\alpha\widehat{\mathbf{H}}(k+1|k))\mathbf{B}\Sigma(k+1|k))\\ &\times\mathbf{I}_N)^{-1}(\widehat{\mathbf{H}}(k+1|k))^H\mathbf{B}^T\mathbf{P}(\alpha\widehat{\mathbf{H}}(k+1|k))\mathbf{A}\mathbf{x}_k. \end{aligned}\tag{14}$$

Proof: See [20, Appendix A]. ■

According to Theorem 2, when $\|\Sigma(k+1|k)\|$ is large, $\mathrm{Tr}\big(\mathbf{B}^T\mathbf{P}(\alpha\widehat{\mathbf{H}}(k+1|k))\mathbf{B}\Sigma(k+1|k)\big)\mathbf{I}_N$ in (14) increases, reducing $\|\mathbf{u}_k^*\|$ and yielding a more conservative action. This reflects a robustness effect against channel uncertainty.

Unlike the LQR algebraic Riccati equation with a fixed matrix $\mathbf{P}$, (12) defines a fixed point over the kernel $\mathbf{P}(\widehat{\mathbf{H}}(k|k-1))$ on the continuous state $\widehat{\mathbf{H}}(k|k-1)$ induced by the Markov channel, making Problem 2 more challenging.

By applying Lyapunov analysis, we obtain the following theorem on plant stability.

Theorem 3 (Plant Stability): Under the sufficient conditions in Theorem 2, the system is stable under $\mathbf{u}_k^*$, i.e., $\limsup_{K\to\infty}\frac{1}{K}\sum_{k=0}^{K-1}\mathbb{E}[\|\mathbf{x}_k\|^2] < \infty$. Furthermore, $\limsup_{K\to\infty}\frac{1}{K}\sum_{k=0}^{K-1}\mathbb{E}[\|\mathbf{x}_k\|^2]$ increases monotonically with the channel prediction MSE $\limsup_{K\to\infty}\frac{1}{K}\sum_{k=0}^{K-1}\mathbb{E}[\mathrm{Tr}(\Sigma(k+1|k))]$.

Proof: See [20, Appendix B]. ■

To compute $\mathbf{u}_k^*$, the kernel $\mathbf{P}(\widehat{\mathbf{H}}(k+1|k))$ must be obtained by solving (12), which suffers from the *curse of dimensionality* since $\widehat{\mathbf{H}}(k+1|k) \in \mathbb{C}^{N\times N}$. To address this, we approximate $\mathbf{P}(\widehat{\mathbf{H}}(k+1|k))$ via discretization based on the statistical structure of the predicted channel. Specifically, under (11), $[\mathbf{H}^c_{k+1}]_{i,i} \sim \mathcal{CN}(0,1)$ as $k\to\infty$. Since the KF prediction $\widehat{\mathbf{H}}(k+1|k)$ concentrates around $\mathbf{H}^c_{k+1}$ with bounded covariance $\Sigma(k+1|k)$, we approximate its distribution by that of $\lim_{k\to\infty}\mathbf{H}^c_{k+1}$. By the three-sigma ($3\sigma$) rule, over 99.7% of the mass lies within a radius-3 disk in the complex plane. We thus quantize each diagonal entry of $\widehat{\mathbf{H}}(k+1|k)$ by partitioning $[0,3]$ into M_r radial levels and $[-\pi,\pi)$ into M_θ angular sectors, with an overflow bin $\mathcal{B}_0$ for magnitudes exceeding 3. The predicted channel gain $\widehat{\mathbf{H}}(k+1|k)$ is then mapped to a bin index $\ell \in \{1, \ldots, L\}$, where $L \triangleq (M_r M_\theta + 1)^N$, corresponding to a quantization region $\mathcal{B}_\ell$. One of these regions is reserved as the overflow region for magnitudes exceeding 3. Each bin $\mathcal{B}_\ell$ is associated with a representative kernel matrix $\bar{\mathbf{P}}_\ell \in \mathbb{S}_+^S$ such that

$$\widehat{\mathbf{H}}(k+1|k) \in \mathcal{B}_\ell \Rightarrow \mathbf{P}(\widehat{\mathbf{H}}(k+1|k)) = \bar{\mathbf{P}}(\widehat{\mathbf{H}}_\ell) = \bar{\mathbf{P}}_\ell, \tag{15}$$

where $\widehat{\mathbf{H}}_\ell \in \mathcal{B}_\ell$ denotes a representative point within bin $\mathcal{B}_\ell$.

By upper-bounding the prior error covariance as $\Sigma(k+1|k) \preceq \bar{\Sigma} = \frac{\sigma_v^2 N}{1-\alpha^2}\mathbf{1}_{|\alpha|<1} + N\mathbf{1}_{|\alpha|=1}$ (Theorem 1), (12) can be approximated by a coupled algebraic Riccati equation

Algorithm 2 Pilot-free Optimal Control

Initialization: Set $\bar{\mathbf{P}}_{i,-1} \in \mathbb{S}_+^S, i \in \{1, 2, ..., L\}$
for $k = 0, 1, \ldots$ **do**
  • **Kernel Update:**
  $\bar{\mathbf{P}}_{\ell,k} = \bar{\mathbf{P}}_{\ell,k-1} + \mu_k(\mathbf{Q} + \mathbf{A}^T\bar{\mathbf{P}}_{\ell',k-1}\mathbf{A} - \mathbf{A}^T\bar{\mathbf{P}}_{\ell',k-1}\mathbf{B}$
  $\times\widehat{\mathbf{H}}_\ell\Big(\widehat{\mathbf{H}}_\ell^H\mathbf{B}^T\bar{\mathbf{P}}_{\ell',k-1}\mathbf{B}\widehat{\mathbf{H}}_\ell + \mathbf{R} + \mathrm{Tr}(\mathbf{B}^T\bar{\mathbf{P}}_{\ell',k-1}$
  $\times\mathbf{B}\bar{\Sigma})\mathbf{I}_N\Big)^{-1}\widehat{\mathbf{H}}_\ell^H\mathbf{B}^T\bar{\mathbf{P}}_{\ell',k-1}\mathbf{A} - \bar{\mathbf{P}}_{\ell,k-1})$
  $\bar{\mathbf{P}}_{\kappa,k} = \bar{\mathbf{P}}_{\kappa,k-1}, \kappa \in \{1, ..., L\} \setminus \ell$
  where $\widehat{\mathbf{H}}(k+1|k)$ is obtained via Algorithm 1.
  • **Control signal generation:**
  $\mathbf{u}_k = -(\mathbf{R} + \widehat{\mathbf{H}}_\ell^H\mathbf{B}^T\bar{\mathbf{P}}_{\ell,k}\mathbf{B}\widehat{\mathbf{H}}_\ell + \mathrm{Tr}(\mathbf{B}^T\bar{\mathbf{P}}_{\ell,k}\mathbf{B}$
  $\times\bar{\Sigma})\mathbf{I}_N)^{-1}(\widehat{\mathbf{H}}_\ell)^H\mathbf{B}^T\bar{\mathbf{P}}_{\ell,k}\mathbf{A}\mathbf{x}_k.$
end for

(CARE) [21] with respect to $\bar{\mathbf{P}}_\ell$, as follows:

$$\bar{\mathbf{P}}_\ell = \mathbf{Q} + \mathbf{A}^T\bar{\mathbf{P}}_{\ell'}\mathbf{A} - \mathbf{A}^T\bar{\mathbf{P}}_{\ell'}\mathbf{B}\widehat{\mathbf{H}}_\ell(\widehat{\mathbf{H}}_\ell^H\mathbf{B}^T\bar{\mathbf{P}}_{\ell'}\mathbf{B}\widehat{\mathbf{H}}_\ell + \mathbf{R} + \mathrm{Tr}(\mathbf{B}^T\bar{\mathbf{P}}_{\ell'}\mathbf{B}\bar{\Sigma})\mathbf{I}_N)^{-1}(\widehat{\mathbf{H}}_\ell)^H\mathbf{B}^T\bar{\mathbf{P}}_{\ell'}\mathbf{A}, \quad (16)$$

where $\bar{\mathbf{P}}_{\ell'} = \bar{\mathbf{P}}(\alpha\widehat{\mathbf{H}}_\ell)$ and $\alpha\widehat{\mathbf{H}}_\ell \in \mathcal{B}_{\ell'}$.

The following theorem establishes the existence of a unique stabilizing solution $\{\bar{\mathbf{P}}_\ell\}_{\ell=1}^L$.

Theorem 4: (*Sufficient Condition for the Existence of a Unique Stabilizing Solution to* (16)) Suppose that, for each ℓ, $(\mathbf{A}, \mathbf{B}\widehat{\mathbf{H}}_\ell)$ is stabilizable and $(\mathbf{A}, \mathbf{Q}^{1/2})$ is detectable. Then, the CARE in (16) admits a unique positive semidefinite stabilizing solution $\{\bar{\mathbf{P}}_\ell^* \succeq 0\}_{\ell=1}^L$ such that $\mathbf{A}+\mathbf{B}\widehat{\mathbf{H}}_\ell\mathbf{K}_\ell(\bar{\mathbf{P}}_\ell^*)$ is Schur for all ℓ, where

$$\mathbf{K}_\ell(\bar{\mathbf{P}}_\ell^*) = -(\mathbf{R} + \widehat{\mathbf{H}}_\ell^H\mathbf{B}^T\bar{\mathbf{P}}_{\ell'}^*\mathbf{B}\widehat{\mathbf{H}}_\ell + \mathrm{Tr}(\mathbf{B}^T\bar{\mathbf{P}}_{\ell'}^*\mathbf{B}\bar{\Sigma})\mathbf{I}_N)^{-1} \times \widehat{\mathbf{H}}_\ell^H\mathbf{B}^T\bar{\mathbf{P}}_{\ell'}^*\mathbf{A}. \quad (17)$$

Proof: See [20, Appendix C]. ∎

Through this mapping, the optimal control solution $\mathbf{u}_k^*$ in (14) can be approximated by $\tilde{\mathbf{u}}_k \in \mathbb{C}^{N\times 1}$, given by

$$\tilde{\mathbf{u}}_k = -(\mathbf{R} + \widehat{\mathbf{H}}_\ell^H\mathbf{B}^T\bar{\mathbf{P}}_{\ell'}^*\mathbf{B}\widehat{\mathbf{H}}_\ell + \mathrm{Tr}(\mathbf{B}^T\bar{\mathbf{P}}_{\ell'}^*\mathbf{B}\bar{\Sigma})\mathbf{I}_N)^{-1} \times \widehat{\mathbf{H}}_\ell^H\mathbf{B}^T\bar{\mathbf{P}}_{\ell'}^*\mathbf{A}\mathbf{x}_k. \quad (18)$$

Consequently, $\mathbf{u}_k^*$ in (13) is approximated by $\tilde{\mathbf{u}}_k$ in (18), reducing the problem to computing the kernel matrices $\{\bar{\mathbf{P}}_\ell\}$ from the CARE in (16). Since the CARE in (16) defines fixed-point equations for $\{\bar{\mathbf{P}}_\ell\}$, these matrices can be computed using an online SA method. The resulting pilot-free optimal control algorithm is summarized in Algorithm 2, whose convergence is established in the following lemma.

Lemma 1 (Convergence of Algorithm 2): Suppose the sufficient condition in Theorem 4 is satisfied, and the step-size sequence $\{\mu_k\}_{k=0}^\infty$ satisfies $\sum_{k=0}^\infty \mu_k = \infty$ and $\sum_{k=0}^\infty \mu_k^2 < \infty$. Then, $\Pr(\lim_{k\to\infty} \mathbf{u}_k = \tilde{\mathbf{u}}_k) = 1$.

Proof: The proof follows similar steps to [9, Appendix C] and is omitted for brevity. ∎

IV. Numerical Results

We evaluate the performance of the proposed pilot-free control framework. The system evolves according to

$$\mathbf{x}_{k+1} = \mathbf{A}\mathbf{x}_k + \mathbf{B}\mathbf{H}_{k+1}^c\mathbf{u}_k + \mathbf{B}\mathbf{n}_k^c + \mathbf{w}_k, \quad (19)$$

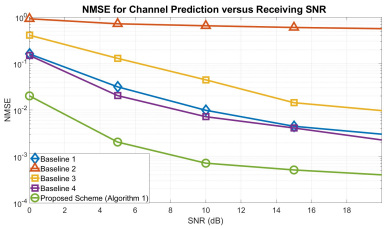

Fig. 2: Normalized MSE (NMSE) of channel prediction versus the received SNR at the dynamic plant.

where

$$\mathbf{A} = \begin{bmatrix} 1.02 & 0.01 & 0 & 0 \\ 0 & 0.02 & 0.05 & 0 \\ 0 & 0 & 0.33 & 0.02 \\ 0.04 & 0 & 0 & 0.21 \end{bmatrix}, \mathbf{B} = \begin{bmatrix} 0.5 & 0 & 0 & 0 \\ 0.1 & 0.6 & 0 & 0 \\ 0 & 0 & 0.7 & 0.21 \\ 0 & 0 & 0 & 0.8 \end{bmatrix}.$$

$\mathbf{w}_k \sim \mathcal{CN}(0, \mathbf{I}_4)$ and $\mathbf{H}_{k+1}^c \in \mathbb{C}^{4\times 4}$ with each non-zero element $h_{i,k}$ evolving according to

$$h_{i,k+1} = 0.95h_{i,k} + 0.3v_{i,k}, \quad (20)$$

where $v_{i,k} \sim \mathcal{CN}(0, 1)$. The quantization parameters are $M_r = M_\theta = 4$.

We consider four baselines for channel prediction. **Baseline 1** uses least-squares (LS) estimation of $\mathbf{H}_k^c$ from $(\mathbf{x}_k, \mathbf{x}_{k-1}, \mathbf{u}_{k-1})$ and assumes $\mathbf{H}_{k+1}^c \approx \mathbf{H}_k^c$. **Baseline 2** performs blind prediction via singular value decomposition (SVD) on state trajectories, extracting dominant structures and similarly assuming $\mathbf{H}_{k+1}^c \approx \mathbf{H}_k^c$. **Baseline 3** extends LS by updating every two slots and interpolating intermediate gains. **Baseline 4** uses pilot-assisted estimation with a unitary pilot matrix and LS at the receiver.

We also benchmark the proposed control policy against four baselines. **Baseline 1** applies the proposed framework with LS-based channel prediction using pilots. **Baseline 2** uses the same control law with interpolation-based channel prediction. **Baseline 3** employs a PID controller based solely on the state $\mathbf{x}_k$, without channel adaptation. **Baseline 4** uses a fixed LQR controller designed offline under nominal conditions, ignoring the time-varying channel $\mathbf{H}_k^c$.

A. Channel Prediction Performance

Fig. 2 shows the NMSE of $\widehat{\mathbf{H}}(k+1|k)$ versus SNR. The proposed Algorithm 1 consistently achieves about one order-of-magnitude lower NMSE than all baselines. Baseline 2 remains nearly flat due to its unsupervised reliance on state trajectories, while Baselines 1 and 4 improve with SNR but ignore temporal correlation Baseline 3 reduces variance via smoothing yet introduces interpolation bias. In contrast, the proposed method exploits structural and temporal dependencies, yielding superior accuracy across all SNR regimes.

B. Control Performance

Fig. 3 shows the averaged plant-state power $\frac{1}{100}\sum_{k=0}^{99}\mathbb{E}[\|\mathbf{x}_k\|^2]$, versus SNR. The proposed method achieves the best performance across all SNRs, with at least 80% reduction over all baselines. Baselines 3 and 4, which

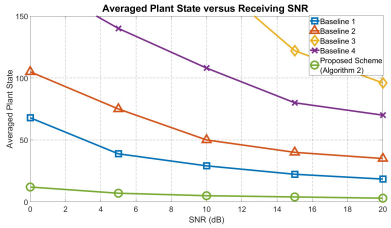

Fig. 3: Averaged plant-state versus the received SNR at the dynamic plant.

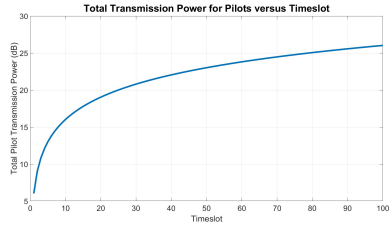

Fig. 4: Cumulative pilot transmission energy versus time slot.

ignore channel knowledge, fail to stabilize the system, while Baselines 1 and 2 remain limited by prediction errors. In contrast, Algorithm 2 leverages accurate channel tracking and structure-aware control, ensuring robust and stable performance across the entire SNR range.

C. Discussion on the Pilot Overhead

Fig. 4 the cumulative pilot transmission energy of the pilot-assisted channel-estimation baseline (channel-prediction Baseline 4). The cumulative pilot energy increases steadily over time, reaching a value corresponding to nearly 25 dB after 100 time slots. In contrast, the proposed pilot-free scheme requires no dedicated pilot transmissions while achieving accurate channel prediction and stable control. This highlights the energy savings of the proposed design relative to pilot-based approaches.

V. Conclusions

In this paper, we proposed a pilot-free control framework enabling real-time optimal control of linear systems over OFDM networks via control-aided channel prediction. A joint optimization problem for channel prediction and control was formulated, where channel prediction was performed using KF and the optimal control policy was derived from the Bellman optimality principle with an SA-based solution to an approximate Riccati equation. We further established joint stability of the channel predictor and system dynamics, and provided sufficient conditions for the existence, uniqueness, and convergence of the proposed solution. Numerical results demonstrated consistent performance gains over conventional baselines across a wide range of SNR regimes in terms of both plant stability and channel prediction accuracy.

Acknowledgment

This work is supported by the SNS JU project 6G-GOALS [22] under the EU's Horizon programme (Grant Agreement No. 101139232). The work of P. A. Stavrou was also supported in part by the Huawei France-EURECOM Chair on Future Wireless Networks.

References

[1] P. Park, S. C. Ergen, C. Fischione, C. Lu, and K. H. Johansson, "Wireless network design for control systems: A survey," *IEEE Commun. Surv. Tutor.*, vol. 20, no. 2, pp. 978–1013, 2017.

[2] X. Wang, J. Zhang, C. Chen, J. He, Y. Ma, and X. Guan, "Trust-AoI-aware codesign of scheduling and control for edge-enabled IIoT systems," *IEEE Trans. Ind. Inform.*, vol. 20, no. 2, pp. 2833–2842, 2023.

[3] Q. Mao, Y. Xu, J. Chen, J. Chen, and T. T. Georgiou, "Maximization of gain/phase margins by PID control," *IEEE Trans. Autom. Control*, vol. 70, no. 1, pp. 34–49, 2024.

[4] A. Ilka and N. Murgovski, "Novel results on output-feedback LQR design," *IEEE Trans. Autom. Control*, vol. 68, no. 9, pp. 5187–5200, 2022.

[5] M. Fink, T. Brüdigam, D. Wollherr, and M. Leibold, "Minimal constraint violation probability in model predictive control for linear systems," *IEEE Trans. Autom. Control*, vol. 69, no. 10, pp. 7043–7050, 2024.

[6] P. A. Stavrou and M. Skoglund, "LQG control and linear policies for noisy communication links with synchronized side information at the decoder," *Automatica*, vol. 123, p. 109306, 2021.

[7] P. K. Mishra, D. Chatterjee, and D. E. Quevedo, "Stabilizing stochastic predictive control under Bernoulli dropouts," *IEEE Trans. Autom. Control*, vol. 63, no. 6, pp. 1579–1590, 2017.

[8] A. Impicciatore, Y. Z. Lun, P. Pepe, and A. D'Innocenzo, "Optimal output-feedback control over Markov wireless communication channels," *IEEE Trans. Autom. Control*, vol. 69, no. 3, pp. 1643–1658, 2023.

[9] M. Tang, S. Cai, and V. K. N. Lau, "Online system identification and control for linear systems with multiagent controllers over wireless interference channels," *IEEE Trans. Autom. Control*, vol. 68, no. 10, pp. 6020–6035, 2022.

[10] Z. Huang, K. Wang, A. Liu, Y. Cai, R. Du, and T. X. Han, "Joint pilot optimization, target detection and channel estimation for integrated sensing and communication systems," *IEEE Trans. Wirel. Commun.*, vol. 21, no. 8, pp. 6294–6309, 2022.

[11] K. Abed-Meraim and N. L. Trung, "Misspecified Cramér–Rao bounds for blind channel estimation under channel order misspecification," *IEEE Trans. Signal Process.*, vol. 69, pp. 1234–1246, 2021.

[12] Z. Zhao and D. Slock, "Decentralized expectation propagation for semi-blind channel estimation in cell-free networks," in *Proc. IEEE Int. Symp. Inf. Theory (ISIT)*, 2024, pp. 2152–2156.

[13] Z. Xiao, S. Cao, L. Zhu, Y. Liu, B. Ning, X.-G. Xia, and R. Zhang, "Channel estimation for movable antenna communication systems: A framework based on compressed sensing," *IEEE Trans. Wirel. Commun.*, vol. 23, no. 1, pp. 123–137, 2024.

[14] X. Ma, Z. Gao, F. Gao, and M. D. Renzo, "Model-driven deep learning based channel estimation and feedback for millimeter-wave massive hybrid MIMO systems," *IEEE J. Sel. Areas Commun.*, vol. 39, no. 8, pp. 2387–2406, 2021.

[15] X. Zheng and V. K. N. Lau, "Online deep neural networks for mmWave massive MIMO channel estimation with arbitrary array geometry," *IEEE Trans. Signal Process.*, vol. 69, pp. 2010–2025, 2021.

[16] S. Cai and V. K. Lau, "Online optimal state feedback control of linear systems over wireless MIMO fading channels," *IEEE Trans. Autom. Control*, vol. 68, no. 7, pp. 4159–4174, 2022.

[17] D. Simon, *Optimal state estimation: Kalman, H infinity, and nonlinear approaches*. John Wiley & Sons, 2006.

[18] D. Bertsekas, *Dynamic programming and optimal control: Volume I*. Athena Scientific, 2012, vol. 4.

[19] A.-A. Lu, X. Gao, W. Zhong, C. Xiao, and X. Meng, "Robust transmission for massive MIMO downlink with imperfect CSI," *IEEE Trans. Commun.*, vol. 67, no. 8, pp. 5362–5376, 2019.

[20] M. Tang, Z. Li, P. A. Stavrou, and M. Kountouris, "Pilot-free optimal control over wireless networks: A control-aided channel prediction approach," *arXiv preprint arXiv:2602.21752*, 2026.

[21] O. L. V. Do Costa, R. P. Marques, and M. D. Fragoso, *Discrete-time Markov jump linear systems*. Springer, 2005.

[22] E. C. Strinati et al., "Goal-oriented and semantic communication in 6G AI-native networks: the 6G-GOALS approach," in *Europ. Conf. on Networks and Commun. & 6G Summit*, June 2024.